

# Aggregation of Descriptive Regularization and Fuzzy Logic Techniques for Enhanced Remote Sensing Imaging

A. Castillo Atoche, O. Palma Marrufo and R. Peon Escalante  
*Facultad de Ingenieria, Universidad Autonoma de Yucatan, Mérida, Mexico*

**Keywords:** Remote Sensing, Parallel Computing, GPUs.

**Abstract:** In this paper, the aggregation of the descriptive regularization and Fuzzy-Logic techniques is proposed for the enhancement/reconstruction of the power spatial spectrum pattern (SSP) of the wave field scattered from remotely sensed scenes. In particular, the Weighted Constrain Least Square (WCLS) and the Fuzzy anisotropic diffusion techniques are algorithmically adapted and implemented in a parallel fashion using commodity graphic processor units (GPUs) improving the time performance of real-time remote sensing applications. Experimental results show the performance efficiency both in resolution enhancement and in computational complexity reduction metrics with the presented approach.

## 1 INTRODUCTION

Advances in sensor technology are revolutionizing the way of images are collected, managed and processed. The incorporation of latest-generation sensors to radar/SAR systems is currently producing a near-continual stream of high-dimensional image data. Such amount of collected information is now required to be processed in (near) real-time mode for newer applications in Earth monitoring, in medical image fusion and enhancement, and computer vision. Relevant examples include monitoring of natural disasters like earthquakes and floods, military applications, tracking of man-induced hazards, forest fires, oil spills and other types of biological agents. Also, these applications need timely responses for swift decision which depend upon real-time performance of algorithm implementation (Henderson and Lewis, 1998),(Chang, 2007), (Goodman et al., 2011), (Yu et al., 2013). Additionally, the computational complexity of the advanced high-resolution remote sensing (RS) and radar imaging techniques that employ the recently developed regularization methods for enhanced radar imaging and remote sensing (RS) image reconstruction/ enhancement procedures (Shkvarko et al., 2008),(Castillo Atoche et al., 2010), (Shkvarko, 2010) is definitively unacceptable for a (near) real-time implementation with any existing digital signal processor (DSP) or high-speed personal computer (PC). In this regard, a tremendous amount of data processing is required to be computed for different type

of image processing algorithms. To provide such high computational demands under (near) real-time constraints, highly parallel processing schemes must be developed. Usually, general-purpose systems are used like multi-PC's, field programmable gate arrays (FPGAs) or digital signal processing (DSP) platforms. Therefore, the implementation of the aggregated descriptive regularization and fuzzy anisotropic diffusion techniques via GPU computing for real-time data processing is considered in this study.

The principal innovation that distinguishes our approach from previous studies (Paz and Plaza, 2010), (Castillo Atoche et al., 2009), (Liu and Plaza, 2011) is twofold: first, the conceptualization and algorithmically aggregation of the weighted constrained least square (WCLS) algorithm with the fuzzy Anisotropic Diffusion technique for image enhancement is employed. In this stage fuzzy edge detectors are introduced in order to provide a more flexible and robust way to define the edges instead of using the well-known Laplacian filter as the edge factor in the anisotropic diffusion. The essential idea is to avoid blurring of the edges, after the WCLS reconstruction, with the incorporation of an edge stopping function which estimates the diffusion coefficients ensuring the smoothing process only in the interior regions without crossing the edges. Second, the algorithmic implementation using massively processors with a graphic processing unit (GPU) platform is performed. Here, parallel computing techniques are used in order to improve the time performance of the algo-

rithm. Simulation analysis and the performance evaluation with the NVIDIA Tesla C2075, are indicative that our GPU-based implementation is also oriented toward real-time remote sensing processing applications.

## 2 PROBLEM STATEMENT

In radar imaging (Henderson and Lewis, 1998), (Shkvarko et al., 2008), the backscattered field of the remotely sensed surface  $X \ni \mathbf{x}$  is modeled by imposing its time invariant complex scattering function  $e(\mathbf{x})$  over the object scene  $X \ni \mathbf{x}$ . The measurement data wavefield  $u(\mathbf{y}) = s(\mathbf{y}) + n(\mathbf{y})$  consists of echo signals  $s$  and additive noise  $n$ , and is available for observations and recordings within the prescribed time-space observation domain  $Y = T \times P$ , where  $\mathbf{y} = (t, \mathbf{p})^T$  defines the time-space points in  $Y$ . The model of the observation wavefield  $u$  is defined by specifying the stochastic equation of observation (EO) of an operator form:  $u = Se + n; e \in E; u, n \in U; S: E \rightarrow U$ , in the Gilbert signal spaces  $E$  and  $U$  with the metric structures induced by the inner products  $[u_1, u_2]_U$  and  $[e_1, e_2]_E$ , respectively.

All the fields  $e, n, u$  are assumed to be zero-mean complex valued Gaussian random fields. An incoherent nature of the backscattered field  $e(\mathbf{x})$  is next assumed, this is naturally inherent to the radar imaging experiments (Henderson and Lewis, 1998), (Shkvarko et al., 2008) and leads to the  $\delta$ -form of the object field correlation function,  $R_e(\mathbf{x}_1, \mathbf{x}_2) = B(\mathbf{x}_1)\delta(\mathbf{x}_1 - \mathbf{x}_2)$ , where  $e(\mathbf{x})$  and  $B(\mathbf{x}) = \langle |e(\mathbf{x})|^2 \rangle$  are referred to as a random complex scattering function of the probing surface and its average power scattering function or spatial spectrum pattern (SSP), respectively.

Next, the conventional finite-dimensional vector form approximation (Castillo Atoche et al., 2010) of the continuous-form EO is taken into account as follows

$$\mathbf{u} = \mathbf{S}\mathbf{e} + \mathbf{n} \quad (1)$$

where  $\mathbf{u}, \mathbf{n}$  and  $\mathbf{e}$  define the vectors composed by the coefficients of the finite-dimensional approximation of the fields  $u, n$  and  $e$ , respectively, and  $\mathbf{S}$  is the matrix-form approximation of the signal formation operator (SFO). The average  $\mathbf{b} = \text{vect} \{ \langle e_k, e_k^* \rangle; k = 1, \dots, K \}$  of the random scattering vector  $\mathbf{e}$  has a statistical meaning of the average power scattering function traditionally referred as the spatial spectrum pattern (SSP), where the asterisk indicates the complex conjugate. This SSP is a second order statistics of the scattered field that represent the brightness reflectivity of the image scene  $\mathbf{B} = L\{\mathbf{b}\}$ ,

represented in a conventional pixel format over the rectangular scene frame (Shkvarko et al., 2008).

The RS imaging problem is stated as follows: to find an estimate of the scene pixel-frame image  $\hat{\mathbf{B}}$  via lexicographical reordering  $\hat{\mathbf{B}} = L\{\hat{\mathbf{b}}\}$  of the spatial spectrum pattern (SSP) vector estimate  $\hat{\mathbf{b}}$  reconstructed from whatever available measurements of independent realizations  $\{u_{(j)}; j = 1, \dots, J\}$  of the recorded data vector.

## 3 DESCRIPTIVE REGULARIZATION STRATEGY

In this section, vector  $\hat{\mathbf{b}}$  is estimated as a discrete-form representation of the desired SSP over the pixel-formatted object scene remotely sensed with an employed array radar/SAR. Thus, one can seek to estimate  $\hat{\mathbf{b}} = \{\hat{\mathbf{R}}_e\}_{diag}$  given the data correlation matrix  $\mathbf{R}_u$  pre-estimated by some means, e.g. via averaging the correlations over  $L$  independent snapshots (Shkvarko, 2010), (Castillo Atoche et al., 2009);  $\hat{\mathbf{R}}_u = \mathbf{Y} = (1/L) \sum_{l=1}^L \mathbf{u}_{(l)} \mathbf{u}_{(l)}^+$ , and by determining the solution operator that we also refer to as the signal image formation operator (SO)  $\mathbf{W}$  such that

$$\hat{\mathbf{b}} = \{\hat{\mathbf{R}}_e\}_{diag} = \{\mathbf{W}\mathbf{Y}\mathbf{W}^+\}_{diag}. \quad (2)$$

To optimize the search of  $\mathbf{W}$ , the following descriptive regularization strategy is proposed

$$\mathbf{W} \longrightarrow \min_{\mathbf{W}} \{\mathfrak{R}(\mathbf{W})\} \quad (3)$$

where

$$\mathfrak{R}(\mathbf{W}) = \text{tr}\{(\mathbf{W}\mathbf{S} - \mathbf{I})\mathbf{A}(\mathbf{W}\mathbf{S} - \mathbf{I})^+\} + \alpha \text{tr}\{\mathbf{W}\mathbf{R}_N\mathbf{W}^+\} \quad (4)$$

implies the minimization of a weighted sum of the systematic and fluctuation errors in the desired estimate  $\hat{\mathbf{b}}$ , where the selection (adjustment) of the regularization parameter  $\alpha$  and the weight matrix  $\mathbf{A}$  provides the additional degrees of freedom incorporating any descriptive properties of a solution if those are known a priori (Shkvarko et al., 2008).

Solving the minimization problem of (3), we obtain

$$\mathbf{W} = \mathbf{K}_{A,\alpha} \mathbf{S}^+ \mathbf{R}_N^{-1}, \quad (5)$$

where

$$\mathbf{K}_{A,\alpha} = (\mathbf{S}^+ \mathbf{R}_N^{-1} \mathbf{S} + \alpha \mathbf{A}^{-1})^{-1} \quad (6)$$

and the desired SSP estimate is given by

$$\hat{\mathbf{b}} = \{\mathbf{K}_{A,\alpha} \mathbf{S}^+ \mathbf{R}_N^{-1} \mathbf{Y} \mathbf{R}_N^{-1} \mathbf{S} \mathbf{K}_{A,\alpha}\}_{diag}. \quad (7)$$

In the case of white noise,  $\mathbf{R}_N^{-1} = (1/N_o)\mathbf{I}$  is considered. Thus, for the case of the proposed weighted

constrained least square (WCLS) algorithm, a modified version of (7) is determined. The following re-adjustments of the degrees of freedom are employed  $\mathbf{A} = \mathbf{M}_B$  and  $\alpha = N_o/b_o$ . Therefore, the WCLS estimator is represented as follows

$$\mathbf{W}_{WCLS} = (\mathbf{S}^+ \mathbf{R}_N^{-1} \mathbf{S} + \alpha \mathbf{M}_B)^{-1} \mathbf{S}^+ \mathbf{R}_N^{-1}. \quad (8)$$

Any other feasible adjustments in the degrees of freedom (the regularization parameter  $\alpha$ , and the weight matrix  $\mathbf{A}$ ) provide other possible SSP reconstruction techniques that are not considered in this study.

## 4 AGGREGATION OF FUZZY ANISOTROPIC DIFFUSION TECHNIQUE

In this section, the aggregation of fuzzy anisotropic diffusion technique is incorporated for the enhanced of remote sensing imaging. First, the diffusion processing technique is considered as the result of convolving the reconstructed remotely sensed image  $\hat{b}_o$  with a Gaussian kernel  $G$  of increasing width as follows

$$\hat{b}(x, y, t) = \hat{b}_o(x, y) * G(x, y, t). \quad (9)$$

Here, (9) acts as a low-pass filter suppressing high frequencies in the image  $\hat{b}$ . The problem is that the image edges and noises are both high frequency signals, and therefore, the edges are blurred by this operation. To solve this problem, the anisotropic diffusion equation proposed in (Song and Tizhoosh, 2003) is next defined as

$$\frac{\partial \hat{b}(\mathbf{r}; t)}{\partial t} = \text{div}(c(\mathbf{r}; t) \nabla \hat{b}(\mathbf{r}; t)), \quad (10)$$

where  $R \ni \mathbf{r} = (x, y)$  for the continuous 2-D rectangular scene frame,  $c(\mathbf{r}; t) = g(\|\nabla \hat{b}(\mathbf{r}; t)\|)$  is the diffusion coefficient where  $g(\cdot)$  is called edge stopping function,  $\nabla \hat{b}$  is the gradient of the image and  $\frac{\partial \hat{b}(\mathbf{r}; t)}{\partial t}$  represents the enhanced SSP estimate  $\hat{b}(\mathbf{r}; t)$  which provides edge preservation in the scene regions with high gradient contrast while performing smoothed windowing over the homogeneous image zones corrupted by Gaussian noise.

Now, the discrete version of the anisotropic diffusion equation of (10) is represented as

$$\begin{aligned} \hat{b}_r^{[i+1]} = \hat{b}_s^{[i]} + \lambda & \left[ \frac{1}{d_x^2} \cdot c_N \cdot D_N(\hat{b}) + \frac{1}{d_x^2} \cdot c_S \cdot D_S(\hat{b}) + \right. \\ & \frac{1}{d_y^2} \cdot c_E \cdot D_E(\hat{b}) + \frac{1}{d_y^2} \cdot c_W \cdot D_W(\hat{b}) + \\ & \frac{1}{d_d^2} \cdot c_{NE} \cdot D_{NE}(\hat{b}) + \frac{1}{d_d^2} \cdot c_{NW} \cdot D_{NW}(\hat{b}) + \\ & \left. \frac{1}{d_d^2} \cdot c_{SE} \cdot D_{SE}(\hat{b}) + \frac{1}{d_d^2} \cdot c_{SW} \cdot D_{SW}(\hat{b}) \right]_r^{[i]} \end{aligned} \quad (11)$$

where  $c_N, c_S, c_E, c_W, c_{NE}, c_{NW}, c_{SE}, c_{SW}$  represents the conduction coefficients,  $d_x, d_y, d_d$  are the distance between pixels and  $D_N, D_S, D_E, D_W, D_{NE}, D_{SE}, D_{NW}, D_{SW}$  indicates the nearest-neighbour differences for the corresponding direction.

In this paper, the conduction coefficients are calculated as follows

$$c_x = \frac{1}{1 + \left(\frac{D_x}{K}\right)^2}. \quad (12)$$

The parameter  $K$  in (12) is chosen according to the noise level and the edge strength. In any remote sensing system, the noise level is not known a priori with certainty (Henderson and Lewis, 1998). Furthermore, because of inherent noise, the calculated edge strength based on gradient is not a true reflection of the edge strength. Therefore, the ambiguity of choosing a suitable value for parameter  $K$ , and thus, the uncertainty in the diffusion coefficient justifies the use of fuzzy set theory in such situations.

In this regard, each nearest-neighbor differences  $D_x$ , that define the edge factor algorithmically same as Laplacian Filter in each direction in the traditional Perona-Malik anisotropic diffusion algorithm, is replaced by a Fuzzy Logic Set (FLS) that calculates the edges in order to avoid the noise of the remote sensing images. The following fuzzy rules are defined

The proposed fuzzy anisotropic diffusion approach is next defined as

$$\begin{aligned} \hat{b}_r^{[i+1]} = \hat{b}_s^{[i]} + \lambda & \left[ \frac{1}{d_x^2} \cdot c_N \cdot \Upsilon_N(\hat{b}) + \frac{1}{d_x^2} \cdot c_S \cdot \Upsilon_S(\hat{b}) + \right. \\ & \frac{1}{d_y^2} \cdot c_E \cdot \Upsilon_E(\hat{b}) + \frac{1}{d_y^2} \cdot c_W \cdot \Upsilon_W(\hat{b}) + \\ & \frac{1}{d_d^2} \cdot c_{NE} \cdot \Upsilon_{NE}(\hat{b}) + \frac{1}{d_d^2} \cdot c_{NW} \cdot \Upsilon_{NW}(\hat{b}) + \\ & \frac{1}{d_d^2} \cdot c_{SE} \cdot \Upsilon_{SE}(\hat{b}) + \\ & \left. \frac{1}{d_d^2} \cdot c_{SW} \cdot \Upsilon_{SW}(\hat{b}) \right]_r^{[i]} \end{aligned} \quad (13)$$

where  $\Upsilon_x$  represents the edge in each direction using a centroid defuzzifier. Now, the design is ready to implement the Fuzzy Anisotropic Diffusion in the GPU platform.

Table 1: Proposed Fuzzy rules.

- $R_1$  IF  $\{D_{NW}$  and  $D_N$  and  $D_{NE}\}$  are Zero then  $\{Black\}$  Else  $\{White\}$ ,
- $R_2$  IF  $\{D_{SW}$  and  $D_S$  and  $D_{SE}\}$  are Zero then  $\{Black\}$  Else  $\{White\}$ ,
- $R_3$  IF  $\{D_{NE}$  and  $D_E$  and  $D_{SE}\}$  are Zero then  $\{Black\}$  Else  $\{White\}$ ,
- $R_4$  IF  $\{D_{NW}$  and  $D_W$  and  $D_{SW}\}$  are Zero then  $\{Black\}$  Else  $\{White\}$ ,
- $R_5$  IF  $\{D_N$  and  $D_{NE}$  and  $D_E\}$  are Zero then  $\{Black\}$  Else  $\{White\}$ ,
- $R_6$  IF  $\{D_N$  and  $D_{NW}$  and  $D_W\}$  are Zero then  $\{Black\}$  Else  $\{White\}$ ,
- $R_7$  IF  $\{D_E$  and  $D_{SE}$  and  $D_S\}$  are Zero then  $\{Black\}$  Else  $\{White\}$ ,
- $R_8$  IF  $\{D_W$  and  $D_{SW}$  and  $D_S\}$  are Zero then  $\{Black\}$  Else  $\{White\}$ .

## 5 GPU IMPLEMENTATION

In this section, the GPU-based implementation of the aggregated WCLS-Fuzzy anisotropic diffusion algorithm is developed. Figure 1 illustrates the flowchart of the proposed system describing the methodology for enhancement of remote sensing imaging. The multicore architecture of the GPU and the employment of textures memories for high-speed access were taken into account in the design. In this study, CUDA kernels were used, which are subroutines callable from the host that execute on the CUDA device. That is, an extern function is called from the host and it calls the different kernels. A kernel employ many threads to perform the specific operation defined in the kernel source code. Moreover, the kernel should make partitions of the data to be processed by each thread, taking care of not overlap threads processing on any memory section in order to avoid undesired

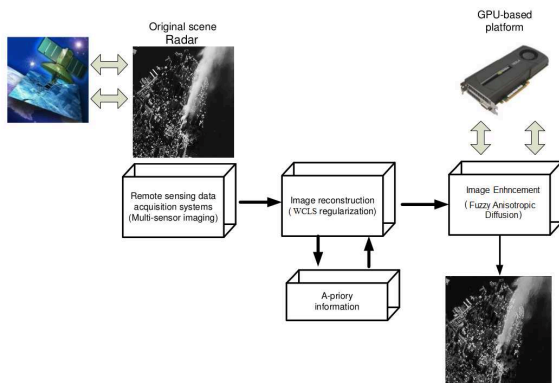


Figure 1: Flowchart describing the methodology adopted for the development of the system.

results. Three different types of data partitioning are identified for image processing: spectral, spatial and mixed, as illustrated in Figure 2. Considering the analysis of the previous WCLS and Fuzzy anisotropic diffusion algorithms, the spatial partition is selected in order to improve the parallelism in the design.

Now, the computational procedures for the implementation of the WCLS reconstructive algorithms are described. First, the device overlap function was activated with the capacity to simultaneously execute a CUDA kernel while performing a copy between CPU to GPU memory (Sanders and Kandrot, 2011). Multiple CUDA streams are created to perform this overlap of computation in data transfer. In addition, the memory configuration management using the *mmap* library of GNU C is employed. Second, the matrix operations of the WCLS algorithm are computed. A specific CUDA kernel is implemented using one grid of  $n \times m$  blocks, in which each block process the corresponding sub-matrix operation in a parallel scheme, and the results are loaded in the shared memory of the GPU. The reduction algorithm is proposed for the implementation of several addition operations in this stage.

For the aggregation of the Fuzzy anisotropic diffusion, a triangular membership function define the fuzzy sets. The Fuzzy sets are initialized using the triangular membership function with the following values,  $White = 147$ ,  $Black = 107$  and  $Zero = 5$ . These Fuzzy sets are allocated in the GPU memory, and the use of *NPP* library is considered, which optimize the functions that work on 1-D and 2-D arrays.

Next, the extern function *PeronaMalik* is called from host, it binds the texture to array, calls the Fuzzy kernel for image enhancement and normalize the resulting array using optimized Nvidia Performace Primitives, i.e., the *nppsMinMax32f* to get the minimum and maximum float value resulting form the Fuzzy kernel, and *nppsNormalize32f* to normalize the image with resulting minimum value at 0 and maximum at 255.

Summarizing, each thread apply the fuzzy rules, deffuzifies the fuzzy set and compute the values for the fuzzy anisotropic diffusion. The fuzzy rules are implemented in the form of minimum function for the conditional part of the rule. The fuzzy sets Black and White are implemented also as minimum functions.

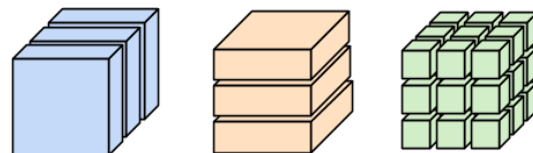


Figure 2: Types of image data partitioning: (a) spectral, (b) spatial and (c) mixed.

Afterwards, the fuzzy sets are defuzzified computing the centroid of them. Finally, the resulting scalar is used on the fuzzy anisotropic diffusion equations.

## 6 SIMULATIONS AND PERFORMANCE ANALYSIS

In order to demonstrate the image enhancement with the proposed approach towards real-time processing, the following simulation experiments are conducted using a real-world satellite image. The tested scene is shown in Fig. 3(a). In the reported simulations, the case of white observation noise (Henderson and Lewis, 1998) is considered with SNR of 20 dB as shown in Fig. 3(b). Fig. 3(c) presents the image enhancement using the Perona-Malik anisotropic diffusion method and Fig. 3(d) shows the image enhancement with the proposed WCLS-fuzzy anisotropic diffusion method.

In the presented performance analysis, the proposed algorithm was implemented in the CPU quad core Intel Xeon E5603 at 1.6 GHz and in the NVIDIA Tesla C2075 GPU platform as well. The results of such comparative analysis are shown in Table 1.

Table 2: Processing time comparative.

Image size (pixels)	Time processing (seconds)	
	CPU	GPU
512 x 512	14.83	0.95
1024 x 1024	43.24	1.75

In this regard, the time performance of the proposed algorithm against the C++ reference implementation have been compared.

Having analyzed Table 1, it is possible to note that the processing time required for the WCLS-fuzzy anisotropic diffusion algorithm implementation has been significantly reduced using GPUs. Such GPU implementation requires 1.75 sec for a 1024 x 1024 pixel-format image instead of the 43.24 secs required using the C++ implementation.

Then, the processing time of the proposed GPU based algorithm is about 27 times less than the conventional CPU implementation.

## 7 CONCLUSIONS

The principal result of this study relates to the GPU-based implementation of the aggregated deterministic regularization and Fuzzy-Logic techniques oriented for high-resolution enhanced of remotely sensed imaging. We have examined that pursuing

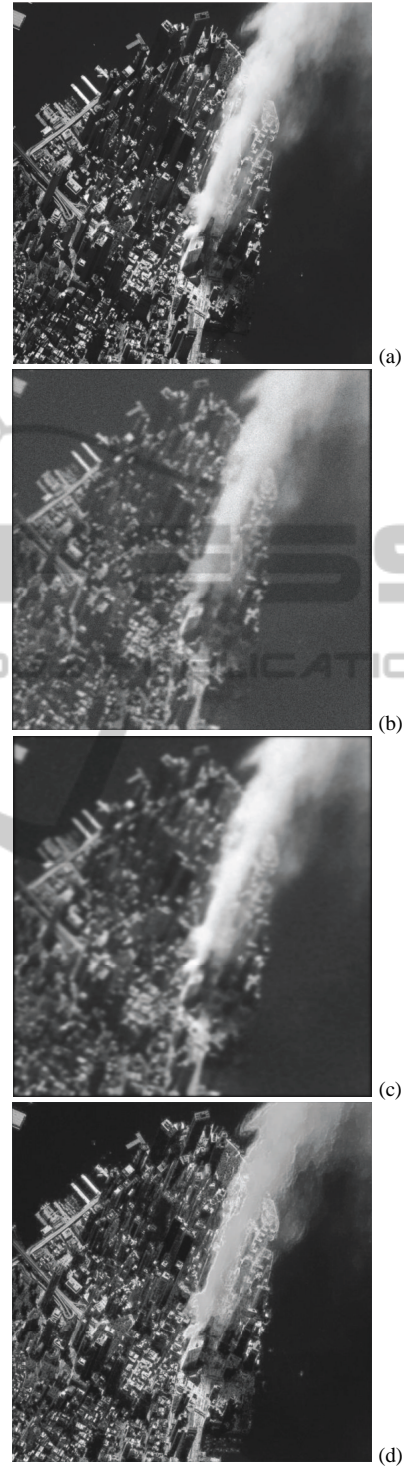


Figure 3: Implementation results: (a) original real-world test scene; (b) degraded scene image formed applying the Matched Space Filter method; (c) image reconstructed applying the WCLS algorithm (4.57 dB); (d) image enhanced applying the WCLS-Fuzzy Anisotropic Diffusion algorithm (9.76 dB).

the proposed GPU computing implementation, the sub-tasks of the WCLS and the Fuzzy-Anisotropic diffusion algorithms can be algorithmically properly adapted in computationally efficient parallel representation towards real-time remote sensing applications. The efficiency of the GPU-based implementation approach was verified with a real test-case scenario in which the time performance of the algorithm was substantially reduced up to 27 orders.

## ACKNOWLEDGEMENTS

This study was supported by Programa de Mejoramiento del Profesorado (PROMEP) and Consejo Nacional de Ciencia y Tecnología (CONACYT) under grants UADY-CA-84 and CB-2010-01-158136, respectively. The authors wish to thank Eduardo Escobar Aquino for his support in running the proposed experiments.

## REFERENCES

Castillo Atoche, A., Shkvarko, Y., Torres Roman, D., and Perez Meana, H. (2009). Convex regularization-based hardware/software co-design for real-time enhancement of remote sensing imagery. *Journal of Real-Time Image Processing*, 4(3):261–272.

Castillo Atoche, A., Torres Roman, D., and Shkvarko, Y. (2010). Experiment design regularization-based hardware/software codesign for real-time enhanced imaging in uncertain remote sensing environment. *EURASIP Journal on Advances in Signal Processing*, 2010:10.

Chang, C.-I. (2007). *Hyperspectral data exploitation: theory and applications*. Wiley-Interscience.

Goodman, J. A., Kaeli, D., and Schaa, D. (2011). Accelerating an imaging spectroscopy algorithm for submerged marine environments using graphics processing units. *Selected Topics in Applied Earth Observations and Remote Sensing, IEEE Journal of*, 4(3):669–6762.

Henderson, F. M. and Lewis, A. J. (1998). *Principles and applications of imaging radar. Manual of remote sensing*. John Wiley and sons, 3rd edition.

Liu, F., S. F. J. and Plaza, A. (2011). Parallel hyperspectral image processing on distributed multicluster systems. *Journal of Applied Remote Sensing*, 5(1).

Paz, A. and Plaza, A. (2010). Clusters versus gpus for parallel target and anomaly detection in hyperspectral images. *EURASIP J. Adv. Signal Process*, 2010:1–18.

Sanders, J. and Kandrot, E. (2011). *CUDA by Example: An Introduction to General-Purpose GPU Programming*. Addison-Wesley Professional, 1st edition.

Shkvarko, Y., Perez-Meana, and Castillo Atoche, A. (2008). Enhanced radar imaging in uncertain environment: a descriptive experiment design regularization

paradigm. *International Journal of Navigation and Observation*, 8:11.

Shkvarko, Y. V. (2010). Unifying experiment design and convex regularization techniques for enhanced imaging with uncertain remote sensing data; part i: Theory. *Geoscience and Remote Sensing, IEEE Transactions on*, 48(1):82–95.

Song, J. and Tizhoosh, H. R. (2003). Fuzzy anisotropic diffusion: A rule based approach. *World Multiconference on Systemics, Cybernetics and Informatics*, pages 241–246.

Yu, J., Liu, A., Yang, Y., and Zhao, Y. (2013). Analysis of sea ice motion and deformation using amsr-e data from 2005 to 2007. *International Journal of Remote Sensing*, 34(12):4127–4141.